Biophysical Chemistry 153 (2010) 36–42

Contents lists available at ScienceDirect

Biophysical Chemistry

journal homepage: http://www.elsevier.com/locate/biophyschem

Large catalase based bioelectrode for biosensor application

Preety Vatsyayan [a], Sandip Bordoloi [b], Pranab Goswami [a,*]

[a] Department of Biotechnology, Indian Institute of Technology Guwahati, Assam, 781039, India
[b] Center for Energy, Indian Institute of Technology Guwahati, Assam, 781039, India

ARTICLE INFO

Article history:
Received 10 August 2010
Received in revised form 23 September 2010
Accepted 4 October 2010
Available online 8 October 2010

Keywords:
Catalase
Direct electrochemistry
Charge transfer resistance
Electrocatalytic activity
Hydrogen peroxide

ABSTRACT

A large catalase (CAT) (Mr ~ 90 kDa), immobilized on multiwalled carbon nanotubes—Nafion® (MWCNT-NF) matrix and encapsulated with polyethylenimine (PEI) on glassy carbon electrode (GCE), showed a pair of nearly reversible cyclic voltammetric peaks for $Fe^{(III)}/Fe^{(II)}$ couple with formal potential of about −0.45 V (vs. Ag/AgCl electrode at pH 7.5). PEI significantly reduced the charge transfer resistance and stabilized the bioelectrode through electrostatic interaction. The electron transfer rate constant and surface coverage of the immobilized CAT were $1.05 \pm 0.2\ s^{-1}$ and 2.1×10^{-10} mol cm^{-2}, respectively. Studies on electrocatalytic activity and kinetics of GCE/MWCNT-NF/CAT/PEI for hydrogen peroxide (H_2O_2) showed the apparent Michaelis–Menten constant of 3 mM, linear response in the range of 10 μM to 5 mM, response time of ~2 s for steady state current, and detection limit of ~1 μM. A high operational and storage stability was also demonstrated for the bioelectrode. Hence, the direct electrochemistry of the large catalase and its potential biosensor application have been established through this investigation.

1. Introduction

Catalase is a heme-containing redox enzyme known for its ability to degrade hydrogen peroxide (H_2O_2) [1]. This catalytic degradation occurs in two-steps: the first step involves the reduction of an H_2O_2 molecule into water with the concomitant oxidation of the catalase heme Fe^{3+} to an oxyferryl species ($Fe^{4+}=O^{+\cdot}$) while the second step involves oxidation of a second molecule of H_2O_2 into water and oxygen with the associated reduction of the oxyferryl species that regenerates the heme Fe^{3+}. Efforts have been made to exploit this functional property of catalase for developing electrochemical biosensors applicable to various industrial niches [2–4].

Studies on the molecular characteristics of catalases from various sources have shown two distinct groups of catalases: small subunit catalases with molecular weight less than 60 kDa and large subunit catalases with molecular weight more than 75 kDa [5]. The high molecular weight contributes to the massive quaternary structure of these large catalase proteins. As example, the masses of the quaternary protein of the large catalases reported from *Aspergillus* strains are more than 360 kDa [6,7]. These large catalases are reported to be highly efficient and stable over a wide range of pH and temperature conditions, more resistant to peroxide damage, enhanced resistance to denaturants, and less sensitive to inactivation by azide than other catalases [7–10]. From the application perspective, the properties of the large catalases are attractive. However, the electrochemical studies on these large enzyme-proteins for their possible biosensor applications are not actively pursued. The reason partly being attributed to the fact that the direct electrical contact between the electrode surfaces and the redox centers of large enzyme-proteins are often inhibited by the thick insulating protein matrix and complex molecular structures [11,12]. The electrochemical studies on enzyme biocatalysts for biosensor or biofuel cell applications are mostly reported on the relatively small redox enzymes like small subunit catalases and other small proteins [13–15].

We report here the direct electrochemistry of a large catalase (CAT) immobilized in a nano-composite matrix on the surface of a glassy carbon electrode (GCE). Multiwalled carbon nanotubes (MWCNT), which has been used previously for fabrication of many enzyme bioelectrodes [16–19] due to its good electrical conductivity, high mechanical strength, and antifouling property [20], was dispersed on the surface of the electrode using hydrophobic polymer chain of Nafion® (NF) following the approach of Wang et al. [21]. Polyethylenimine (PEI), a polycationic polymer [22], was used as an encapsulating material for the immobilization of the CAT on this nano-matrix coated on GCE. PEI has been previously used for other enzymes in combination with MWCNT [23–25] mostly for its dispersion properties. Our aim of utilizing PEI is to exploit the electrostatic interactions between the negatively charged underlying layer of MWCNT-NF/CAT (CAT is negatively charged in the buffer above its *pI*) and the positively charged PEI layered over the surface of the enzyme for stabilizing the CAT from leaching. We have observed that the PEI layer provides an excellent stability to the enzyme on the bioelectrode. The fabricated bioelectrode using this large catalase has been characterized and an account on the findings is presented here.

* Corresponding author. Tel.: +91 361 2582202; fax: +91 361 2582249.
E-mail address: pgoswami@iitg.ernet.in (P. Goswami).

0301-4622/$ – see front matter © 2010 Elsevier B.V. All rights reserved.
doi:10.1016/j.bpc.2010.10.002

2. Experimental

2.1. Reagents

CAT (EC 1.11.1.6) was isolated, purified and characterized from *Aspergillus terreus* MTCC 6324 similar to the procedure described elsewhere [7] and was found to be homotetrameric with a subunit molecular weight of ~90 kDa, acidic *pI* ~4.2, high specific activity of $66.00 \pm 3.97 \times 10^5$ U mg^{-1} protein (in 50 mM sodium phosphate buffer, pH 7.5 at room temperature) and high pH and temperature stability, similar large catalases obtained from other fungal sources [7–9,26]. MWCNT (10–15 nm outer diameter, 2–6 nm inner diameter and 0.1–10 μm length) and PEI were obtained from Sigma, NF from Du Pont (USA), and H_2O_2 (30%) was obtained from Merck. 50 mM sodium phosphate buffer (SPB), pH 7.5 was used throughout the experiment. The stock solutions of CAT and bovine serum albumin (BSA) (1 mg ml^{-1}) were prepared by dissolving the lyophilized protein in 50 mM SPB. All solutions were prepared with deionized water (Milli Q). Solutions were de-aerated by bubbling high-purity (99.99%) argon gas through them prior to the experiments, and the electrochemical cell was kept under argon gas atmosphere throughout the experiments.

2.2. Fabrication of MWCNT-NF/CAT/PEI modified GCE and apparatus

Prior to the surface modification, the GCE (5 mm diameter) was polished with 3 μm alumina slurry, and then ultrasonically cleaned successively in distilled water and ethanol to remove adsorbed alumina particles and finally, air dried. The MWCNT-NF film was prepared by a method described by others [27]. Briefly, 10 mg MWCNT was added to 1 ml of 5% NF and sonicated for about 3.5 h to obtain a stable and uniform suspension. 10 μl of this suspension was layered on GCE and allowed to dry under clean air at room temperature. Once dried, 15 μl of CAT solution (0.5 mg ml^{-1}) was layered on the MWCNT-NF nano-composite and kept overnight at 4 °C. Finally, 5 μl of PEI (10%) was layered and dried at room temperature. Separate GCE with each layer as control were prepared simultaneously and dried as described above. Electrochemical experiments were performed with a computer-controlled electrochemical system (AUTOLAB PGSTAT 302N, Eco Chemie B.V., The Netherlands), driven with GPES, FRA and NOVA Softwares. A conventional three-electrodes cell was used with an Ag/AgCl/saturated KCl reference electrode, a platinum wire as counter electrode, and a glassy carbon disk (modified and unmodified) as working electrode. All experiments were carried out at room temperature.

2.3. Stability studies of the fabricated bioelectrode

To determine the effect of PEI layer on bioelectrode stability, leaching studies were carried out in the presence and absence of the PEI layer. GCE/MWCNT-NF/CAT and GCE/MWCNT-NF/CAT/PEI were stored separately in equal volumes of SPB (pH 7.5) at 4 °C and the residual current was measured at −480 mV (the peak potential for CAT electrocatalytic current as determined from above studies) at different time intervals. After each reading the electrodes were shifted to fresh storage buffer to avoid any re-adsorption of CAT on the electrode surface. Aliquots of the storage buffer were taken before each reading and checked for their protein content by Bradford's method [28]. For the determination of operational stability, the bioelectrode was kept in operating condition at −480 mV and current generated was recorded for 48 h. For storage stability, the bioelectrode was stored at 4 °C and residual current was measured at different time intervals. A fixed substrate concentration (1 mM H_2O_2) was used throughout the experiments for all stability studies.

2.4. Energy dispersive X-ray spectroscopy (EDX) study

GCE fabricated with each layer were mounted on the specimen holders with electro-conductive tape and coated with gold under vacuum in a sputter coater (SC 7620 Polaron Range). The elemental analysis was done using an LEO 1430 VP (variable pressure) scanning electron microscope equipped with INCA Oxford EDX facility.

3. Results and discussion

3.1. Characterization of the GCE/MWCNT-NF/CAT/PEI bioelectrode

3.1.1. EDX characterization of fabricated bioelectrode

EDX measurements were performed to obtain the elemental composition of the assembled films on the electrode surface in the stepwise course in order to confirm the immobilization of each layer. Fig. 1 presents the EDX scans of the surfaces of GCE (A), GCE/MWCNT-NF (B), GCE/MWCNT-NF/CAT (C), and GCE/MWCNT-NF/CAT/PEI (D) in the range of 0–10 kV. GCE surface shows only C (Fig. 1A). The main elements of GCE/MWCNT-NF surface are C and F, where C is from GCE, MWCNT and NF whereas, F stems from NF. Other trace elements O and S are also visible in the spectrum (Fig. 1B). The observed elements Fe and N in Fig. 1C are due to the assembly of CAT on the MWCNT-NF modified GCE. The assembly of PEI on the GCE/MWCNT-NF/CAT film can be further demonstrated by the elements C and N stemming from PEI and underlying layers and a reduced but marked presence of Fe and F from CAT and NF layers, respectively in the EDX survey scan of modified electrode surface (Fig. 1D).

3.1.2. Electrochemical impedance spectroscopy (EIS) characterization of fabricated bioelectrode

EIS, which has been identified as a valuable tool for characterizing the surface modifications during immobilization of the protein and other biomolecules on the electrode surface [29], was employed to investigate the electrode surfaces in the modification steps. Fig. 2A shows the results of the EIS at bare GCE, GCE/MWCNT-NF, GCE/PEI, GCE/MWCNT-NF/CAT, GCE/MWCNT-NF/CAT/PEI in the presence of equimolar $Fe(CN)_6^{3-/4-}$. The spectra are presented in the form of Nyquist plots (where Z_{re} is the real and Z_{im} is the imaginary part of impedance) using FRA software of Autolab systems and are overlaid to pinpoint the differences in charge transfer resistance (R_{ct}) with subsequent modification layers. An ideal Nyquist plot reveals the semicircle with the diameter, corresponding to the R_{ct}, which exhibits the electron transfer kinetics of the redox-probe at the electrode interface [29]. As shown in Fig. 2A, a very low R_{ct} was observed for $Fe(CN)_6^{3-/4-}$ at bare GCE (170 Ω). When MWCNT-NF was layered on the electrode surface, R_{ct} increased to about 960 Ω. The increased R_{ct} implies the increased interfacial resistance due to the assembly of MWCNT-NF layer. Interestingly, addition of CAT onto the MWCNT-NF layer decreased the R_{ct} to 500 Ω. A control experiment using BSA instead of CAT in the similarly assembled electrode however showed increase in R_{ct} to 1500 Ω (Fig. 2B). These R_{ct} values though obtained from a single set of experiments, were found to be fairly reproducible as the data obtained in the subsequent repeated experiments fell within ±3% of the corresponding datum presented above. The R_{ct} data infer that adsorption of CAT in the MWCNT-NF layer facilitates the charge transfer across this composite matrix to the GCE. Notably, large catalases have more channels from the protein surface to the redox center than the small catalases or many other proteins. These channels are utilized for access and vent of substrate and dioxygen, respectively, from the redox center [30]. This unique porous morphological property of this large catalase may support its suitable interactions with the underlying nanotubes matrix which may contribute to the increased charge transfer through the bioelectrode. Addition of PEI on the MWCNT-NF/CAT composite further reduces the R_{ct} to 280 Ω. It is expected that the PEI, which is a

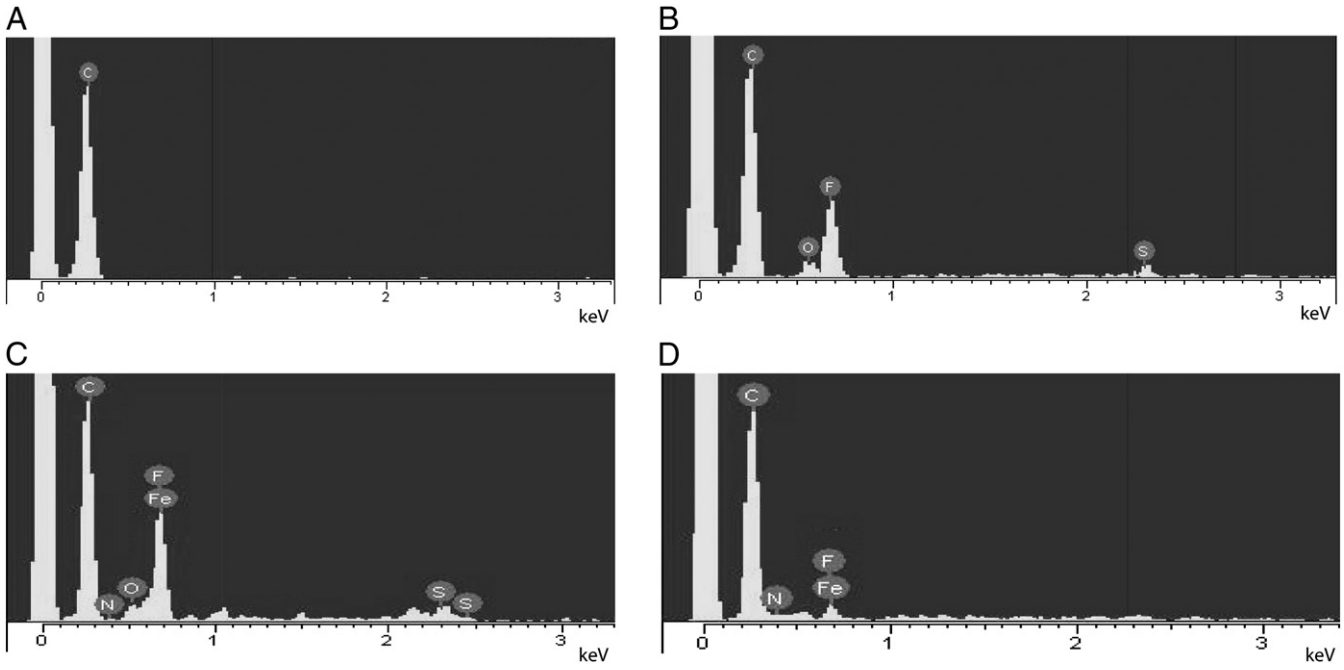

Fig. 1. EDX spectra for layer by layer fabrication of CAT bioelectrode. (A) Bare GCE, (B) GCE/MWCNT-NF, (C) GCE/MWCNT-NF/CAT and (D) GCE/MWCNT-NF/CAT/PEI.

polycation, neutralizes the negative charges developed by the composite MWCNT-NF/CAT (*pI* 4.2) and thereby reduces the charge repulsion between the negatively charged NF and CAT resulting further decrease in the R_{ct} of the bioelectrode. Thus, composite MWCNT-NF/CAT/PEI films on the electrode surface provide facile electron transfer which is also supported by the cyclic voltammetry (CV) results (Fig. 3A, B).

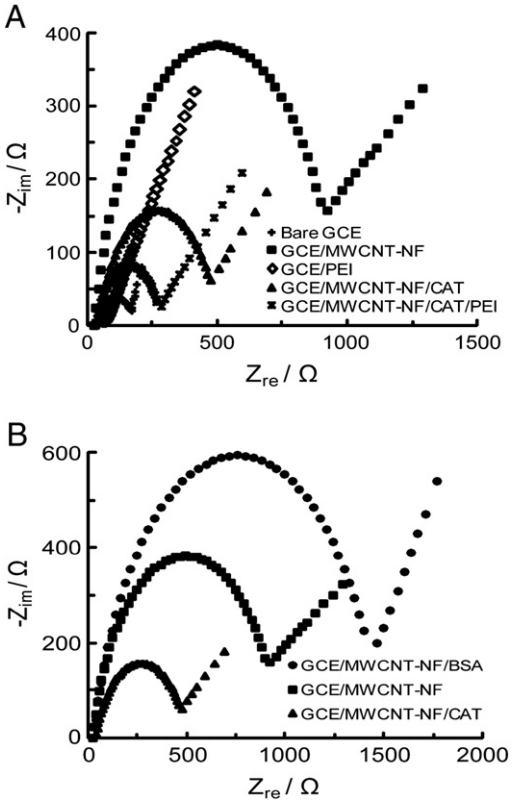

Fig. 2. Electrochemical impedance plots of (A) bare GCE, GCE/MWCNT-NF, GCE/PEI, GCE/MWCNT-NF/CAT and GCE/MWCNT-NF/CAT/PEI; (B) GCE/MWCNT-NF/BSA, GCE/MWCNT-NF and GCE/MWCNT-NF/CAT in the presence of 5 mM $Fe(CN)_6^{3-/4-}$ with 0.1 M KCl as supporting electrolyte. The electrode potential was 0.2 V, the frequency range was 0.1 Hz to 100 KHz.

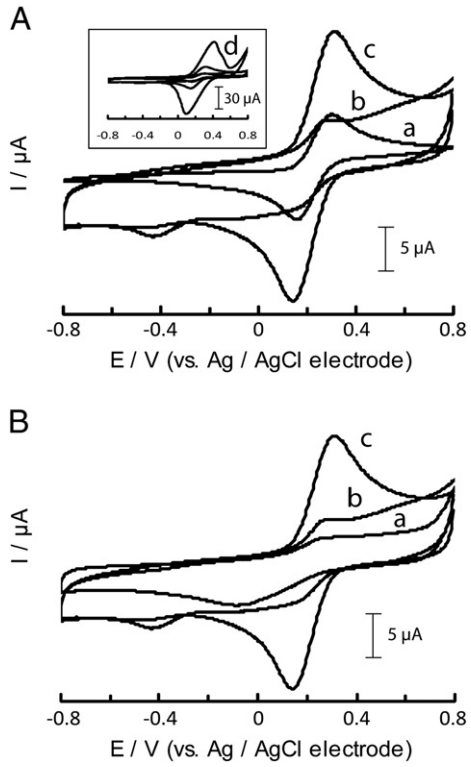

Fig. 3. Cyclic voltammograms of (A) bare GCE (a), GCE/MWCNT-NF (b), GCE/MWCNT-NF/CAT (c) and Inset: GCE/MWCNT-NF/CAT/PEI (d); (B) GCE/MWCNT-NF/BSA (a), GCE/MWCNT-NF (b) and GCE/MWCNT-NF/CAT (c) in the presence of 5 mM $Fe(CN)_6^{3-/4-}$ with 0.1 M KCl as supporting electrolyte.

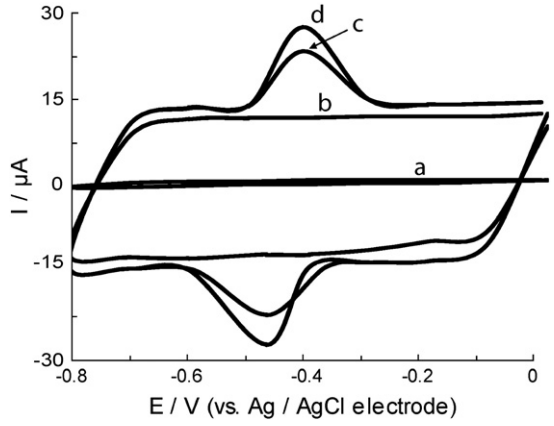

Fig. 4. Cyclic voltammograms of bare GCE (a), GCE/MWCNT-NF (b), GCE/MWCNT-NF/CAT (c) and GCE/MWCNT-NF/CAT/PEI (d) in 50 mM SPB (pH 7.5) at the scan rate of 100 mV s^{-1}.

3.2. Cyclic voltammetry of MWCNT-NF/CAT/PEI modified GCE

The electrochemical behavior of CAT in MWCNT-NF/PEI film was studied by CV. A quasi-reversible CV peak at approximately −0.45 V $[(E_{pa}+E_{pc})/2]$, which is the characteristic of catalase heme $Fe^{(III)}/Fe^{(II)}$ redox couple [31] was observed when MWCNT-NF/CAT electrode was used (Fig. 4, curve c). Free CAT in SPB (pH 7.5) showed no CV peaks at bare GCE in the same potential window. On the other hand, as shown in Fig. 4 (curve d) both cathodic and anodic peak currents increased with the addition of PEI layer. The ratio of anodic to cathodic peak currents is approximately 1.0, indicating that CAT undergoes a quasi-reversible redox process at the GCE modified with MWCNT-NF/CAT/PEI film. MWCNT-NF film provides a well graphitized three-dimensional nano-electrode ensemble for sufficient adsorption of CAT and a suitable environment for electron transfer with underlying GCE. The polycationic layer of PEI further adds to the rate of electron transfer by electrostatic interaction with the CAT (negatively charged, *pI* 4.2) adsorbed on MWCNT-NF film evident from the increase in peak current, although there is no significant shift in the formal potential. The formal potential (E°) of CAT estimated as a midpoint of CV reduction and oxidation peak potentials at approximately −420 and −480 mV, respectively is comparable to the catalase formal potential from other modified electrodes [31–35]. The separation of cathodic and anodic peak potentials ($\Delta Ep = 60$ mV) indicates a single electron transfer reaction. The surface coverage (Γ) of electroactive CAT at the modified GCE was calculated to be 2.1×10^{-10} mol cm^{-2}, by using the equation $\Gamma = Q/nFA$, where Q is the charge obtained by integrating the peak current area, n is the number of electrons involved, F is Faraday's constant and A is electrode area. The calculated Γ is higher than the other reports on the bioelectrodes fabricated with a small catalase on MWCNT-NF-based or other matrix [36,37], suggesting the induction of high level of electroactivity of the immobilized CAT in the matrix of the fabricated bioelectrode. The charge transfer from this homotetrameric CAT protein bearing redox centre in each subunit to the electrode is expected to be facilitated by the cohesive effect of the MWCNT and strong electrostatic interaction between the PEI, a polycationic polymer, and the underlying negatively charged MWCNT-NF/CAT composite matrix that stabilizes the CAT by neutralizing the repulsive interaction between the negatively charged CAT and NF as stated above. To obtain the kinetic parameters of CAT redox at MWCNT-NF/PEI modified GCE, the effect of scan rate was investigated. Fig. 5 shows the CVs at different scan rates. The peak currents (*Ipa* and *Ipc*) versus scan rate plots, shown in the inset (a) of Fig. 5, exhibit a linear relationship ($R^2 = 0.998$ and 0.996, respectively), as expected for a surface-confined redox process. The peak-to-peak separation is approximately 60 mV at scan rates less than 50 mV s^{-1}, suggesting uniform charge transfer kinetics over this range of sweep rates. On the other hand, it was found that at scan rates greater than 100 mV s^{-1}, ΔEp increased with the increasing scan rates. The values of peak-to-peak potential separations were proportional to the logarithm of the scan rate for scan rates greater than 100 mV s^{-1} (inset b of Fig. 5). Based on the Laviron's theory, the transfer coefficient (α) and heterogeneous electron transfer rate constant (k_s) could be estimated by measuring the variation of peak potentials with scan rates [38]. The α and k_s of CAT were 0.7 ± 0.1 and 1.05 ± 0.2 s^{-1}, respectively. Similar k_s values were reported for smaller catalase (bovine liver) immobilized on other electrodes [39,40]. Thus, by following the current protocol, we are reporting here for the first time, an efficient electrical conductivity between the redox centre of large catalase and electrode.

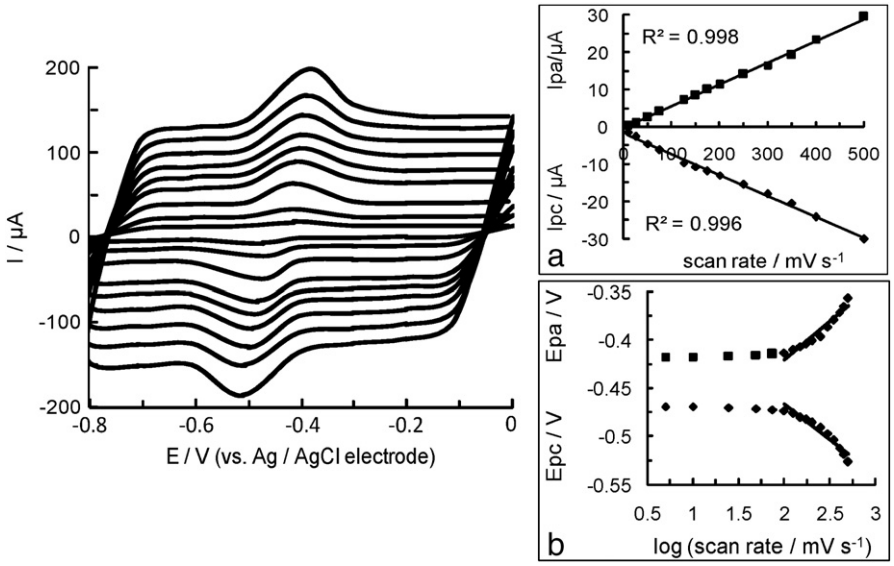

Fig. 5. Cyclic voltammograms of MWCNT-NF/CAT/PEI modified GCE at different scan rates in 50 mM SPB (pH 7.5). The scan rates were 10 to 500 mV s^{-1}. Inset: (a) Plot of peak currents vs. scan rates and (b) Variation of peak potentials vs. the logarithm of the scan rates.

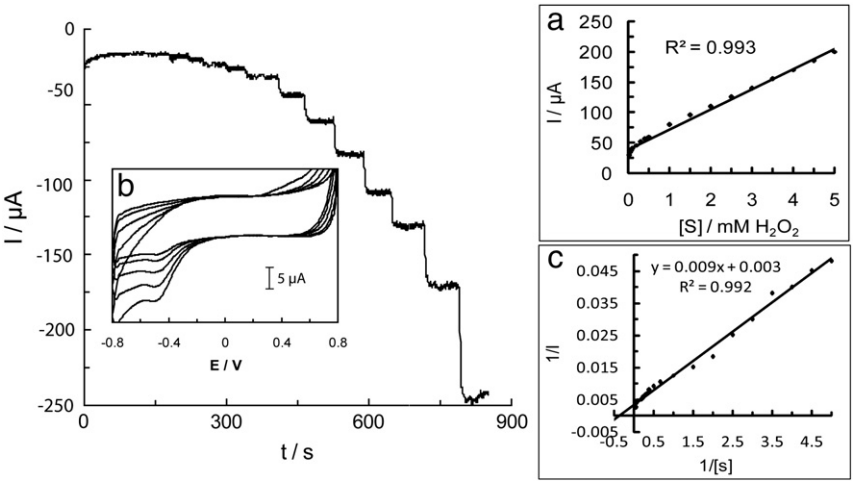

Fig. 6. Chronoamperometric response of GCE/MWCNT-NF/CAT/PEI bioelectrode at different H_2O_2 concentrations. The operating conditions were: −0.48 V (vs. Ag/AgCl electrode), 50 mM SPB (pH 7.5). Inset: (a) Response curve of fabricated CAT bioelectrode. (b) CVs of MWCNT-NF/CAT/PEI modified GCE with successive addition of substrates (ranging from 0.1 to 0.5 mM H_2O_2). (c) Linear calibration curve for the determination of k_m' of immobilized CAT.

3.3. Electrocatalytic behavior of CAT immobilized on MWCNT-NF/PEI modified GCE

The heme in the redox centre of the CAT could be oxidized by H_2O_2 to form an oxyferryl π-cation radical heme intermediate. Subsequently, the enzyme is converted back to its native resting state, ferric porphyrin, by taking electrons from the electrode. The current obtained from the reduction of oxyferryl π-cation radical heme intermediate is correlated to the concentration of H_2O_2 in the solution [41]. Hence, this current can be used to quantify the peroxidase activity of the immobilized CAT system using chronoamperometry. This approach enables the direct measurement of the current versus time response to an applied potential [42]. Fig. 6 shows the real-time chronoamperometric current vs. time curve with subsequent addition of H_2O_2. The current response increases with each addition of H_2O_2 in the testing solution and reaches equilibrium with a response time of ~2 s. A linear response curve ($R^2 = 0.993$) was obtained within the H_2O_2 concentrations from 10 μM to 5 mM with sensitivity 30 μA mM^{-2} H_2O_2 (Fig. 6 inset a). The detection limit of ~1 μM was observed with the constructed biosensor. This low range of substrate concentration, which is much below the saturation range, was considered to measure the kinetic values safely to avoid any possible enzyme inactivation caused by the oxidative stress of the substrate H_2O_2. The apparent Michaelis–Menten constant (k_m') for CAT immobilized on GCE/MWCNT-NF/PEI was 3 mM as determined from the linear calibration plot ($R^2 = 0.975$) (Fig. 6 inset c), where $1/i = 1/i_{max} + k_m'/i_{max}\,C$. The k_m' (3 mM) of fabricated bioelectrode is lower than the biochemically reported k_m values for other large catalases [9] which again suggest the role of MWCNT and PEI in facilitating the electron transfer between substrate and the fabricated bioelectrode. When H_2O_2 was added to the buffer solution, the voltammetric behavior of the CAT-immobilized MWCNT-NF/PEI modified GCE changes obviously, with an increase in the reduction peak current and the disappearance of the oxidation peak, where, the reduction peak current increases with the increasing concentration of H_2O_2 in solution (Fig. 6 inset b). The disappearance of the oxidation peak shows that the oxidation rate of CAT by H_2O_2 is very fast, and increase in reduction peak current indicates the electrocatalytic reduction of CAT immobilized on GCE/MWCNT-NF/PEI. Further, the response time and detection limit of the CAT bioelectrode are comparable and even lower than the bioelectrodes fabricated with smaller catalases [36,37,43,44]. Similarly, the sensitivity of the CAT bioelectrode was also found to be higher than some of the reported small catalase bioelectrodes [37,44]. The remarkably short response time also implies very low diffusion barrier for the substrate and facile charge transfer between the redox center of CAT and the electrode.

3.4. Stability studies for GCE/MWCNT-NF/CAT/PEI bioelectrode

Fig. 7A shows the effect of encapsulating layer of PEI on the stability of CAT bioelectrode towards leaching in buffer. Although, MWCNT-NF composite provides a well defined structure for the surface adsorption

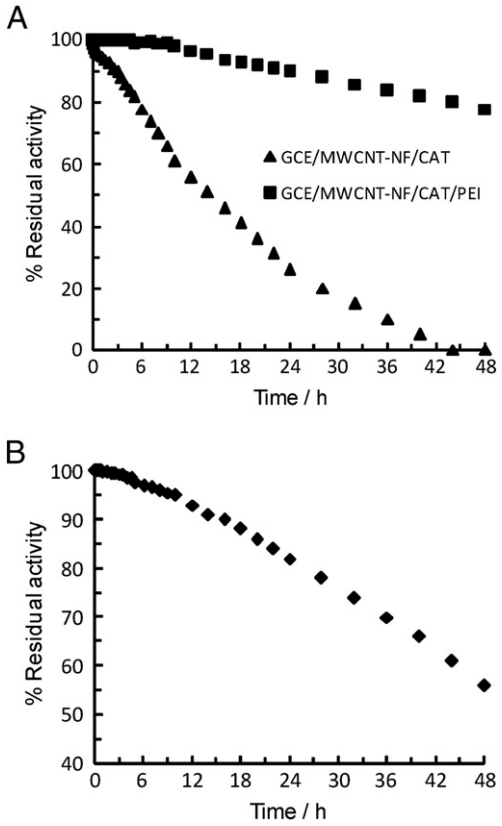

Fig. 7. Stability studies of fabricated CAT bioelectrode. (A) Comparison of stability against leaching for GCE/MWCNT-NF/CAT and GCE/MWCNT-NF/CAT/PEI electrode at 4 °C in 50 mM SPB (pH 7.5). (B) Operational stability of GCE/MWCNT-NF/CAT/PEI electrode. 100% activity corresponds to 80 μA current at substrate concentration of 1 mM H_2O_2 in 50 mM SPB (pH 7.5). The operating conditions were: −0.48 V (vs. Ag/AgCl electrode), 50 mM SPB (pH 7.5). Total number of operations: 25.

of CAT but a complete loss of activity for GCE/MWCNT-NF/CAT bioelectrode within 48 h of leaching studies shows that the composite matrix alone is not able to hold the surface adsorbed CAT for a longer time. In contrast, with the addition of the PEI layer more than 75% of the CAT activity was retained even after 48 h of study, which suggests that PEI provides the encapsulation for surface-confined CAT and prevents its leaching from the bioelectrode. It also improves the stability of bioelectrode by neutralizing the charge repulsion between the negatively charged MWCNT-NF and CAT and by making the electrostatic interaction with the underlying layer. The results of activity studies for the bioelectrode leaching were further supported by the constant presence of much higher concentrations of protein in storage buffer aliquots from GCE/MWCNT-NF/CAT electrode as compared to negligible protein concentrations in the storage buffer aliquots from GCE/MWCNT-NF/CAT/PEI electrode. More than 50% of the CAT residual activity was retained when the GCE/MWCNT-NF/CAT/PEI electrode was continuously operated at −480 mV at room temperature for 48 h at fixed substrate concentration (Fig. 7B). The loss of CAT activity can be attributed to the continuous exposure to high H_2O_2 concentration, effect of temperature and slow leaching of CAT in the solution. The biosensor can be stored for months in dry condition with intermittent use without any significant loss of activity. The high stability of the biosensor in turn is attributed by both innate stability of large CAT and an efficient immobilization technique. Thus, the stability of fabricated CAT bioelectrode also provides it an edge over the other smaller catalase bioelectrodes [15].

4. Conclusions

In this study, direct electrochemistry of a large catalase (CAT) from *A. terreus* immobilized on GCE/MWCNT-NF and encapsulated with PEI was established. This heme protein substantially reduced the R_{ct} of the MWCNT-NF modified GCE. PEI was identified as effective encapsulating polycationic polymer for the large catalase due to its effect on reducing the R_{ct} and increasing the stability of the fabricated bioelectrode. High operational and storage stability of the bioelectrode fabricated following the current immobilization technique were obtained. The values on sensitivity, response time and detection limit obtained by using the bioelectrode towards the substrate H_2O_2 were comparable to or even improved than many reports on small catalases, hence demonstrating the application potential of the large catalase for developing electrochemical biosensor.

Acknowledgement

This work was carried out with the financial support from the Department of Biotechnology (DBT), Government of India.

References

[1] M. Zamocky, F. Koller, Understanding the structure and function of catalases: clues from molecular evolution and *in vitro* mutagenesis, Prog. Biophys. Mol. Biol. 72 (1999) 19–66.
[2] L. Campanella, R. Roversi, M.P. Sammartino, M. Tomassetti, Hydrogen peroxide determination in pharmaceutical formulations and cosmetics using a new catalase biosensor, J. Pharmaceut. Biomed. 18 (1998) 105–116.
[3] L.D. Mello, L.T. Kubota, Biosensors as a tool for the antioxidant status evaluation, Talanta 72 (2007) 335–348.
[4] B. Modrzejewska, A.J. Guwy, R. Dinsdale, D.L. Hawkes, Measurement of hydrogen peroxide in an advanced oxidation process using an automated biosensor, Water Res. 41 (2007) 260–268.
[5] P. Chelikani, I. Fita, P.C. Loewen, Diversity of structures and properties among catalases, Cell. Mol. Life Sci. 61 (2004) 192–208.
[6] K. Kikuchi-Torii, S. Hayashi, H. Nakamoto, S. Nakamura, Properties of *Aspergillus niger* catalase, J. Biochem. 92 (1982) 1449–1456.
[7] J.A. Calera, J. Sanchez-Weatherby, R. Lopez-Medrano, F. Leal, Distinctive properties of the catalase B of *Aspergillus nidulan*, FEBS Lett. 475 (2000) 117–120.
[8] A. Diaz, P. Rangel, Y. Montes De Oca, F. Lledias, W. Hansberg, Molecular and kinetic study of catalase-1, a durable large catalase of *Neurospora crassa*, Free Radic. Bio Med. 31 (2001) 1323–1333.
[9] J. Switala, P.C. Loewen, Diversity of properties among catalases, Arch. Biochem. Biophys. 401 (2002) 145–154.
[10] O.M. Lardinois, P.G. Rouxhet, Peroxidatic degradation of azide by catalase and irreversible enzyme inactivation, Biochim. Biophys. Acta Protein Struct. Mol. Enzymol. 1298 (1996) 180–190.
[11] L. Murphy, Biosensors and bioelectrochemistry, Curr. Opin. Chem. Biol. 10 (2006) 177–184.
[12] R.A. Bullen, T.C. Arnot, J.B. Lakeman, F.C. Walsh, Biofuel cells and their development, Biosens. Bioelectron. 21 (2006) 2015–2045.
[13] N. Hu, Direct electrochemistry of redox proteins or enzymes at various film electrodes and their possible applications in monitoring some pollutants, Pure Appl. Chem. 73 (2001) 1979–1991.
[14] T. Lotzbeyer, W. Schuhmann, H.L. Schmidt, Electron transfer principles in amperometric biosensors: direct electron transfer between enzymes and an electrode surface, Actuat. B 33 (1996) 50–54.
[15] P.A. Prakash, U. Yogeswara, S.M. Chen, A review on direct electrochemistry of catalase for electrochemical sensors, Sensors 9 (2009) 1821–1844.
[16] L. Agui, P. Yanez-Sedeno, J.M. Pingarron, Role of carbon nanotubes in electroanalytical chemistry: a review, Anal. Chim. Acta 622 (2008) 11–47.
[17] J.J. Gooding, Nanostructuring electrodes with carbon nanotubes: a review on electrochemistry and applications for sensing, Electrochim. Acta 50 (2005) 3049–3060.
[18] C. Fu, W. Yang, X. Chen, D.G. Evans, Direct electrochemistry of glucose oxidase on a graphite nanosheet-Nafion composite film modified electrode, Electrochem. Commun. 11 (2009) 997–1000.
[19] J.X. Wang, M.X. Li, Z.J. Shi, N.Q. Li, Z.N. Gu, Direct electrochemistry of cytochrome c at a glassy carbon electrode modified with single-wall carbon nanotubes, Anal. Chem. 74 (2002) 1993–1997.
[20] M. Musameh, J. Wang, A. Merkoci, Y. Lin, Low-potential stable NADH detection at carbon-nanotube-modified glassy carbon electrodes, Electrochem. Commun. 4 (2002) 743–746.
[21] J. Wang, M. Musameh, Y. Lin, Solubilization of carbon nanotubes by nafion toward the preparation of amperometric biosensors, J. Am. Chem. Soc. 125 (2003) 2408–2409.
[22] D. Rochefort, L. Kouisni, K. Gendron, Physical immobilization of laccase on an electrode by means of poly(ethyleneimine) microcapsules, J. Electroanal. Chem. 217 (2008) 53–63.
[23] M.D. Rubianes, G.A. Rivas, Dispersion of multi-wall carbon nanotubes in polyethylenimine: a new alternative for preparing electrochemical sensors, Electrochem. Commun. 9 (2007) 480–484.
[24] A.S. Arribas, E. Bermejo, M. Chicharro, A. Zapardiel, G.L. Luque, N.F. Ferreyra, G.A. Rivas, Analytical applications of glassy carbon electrodes modified with multi-wall carbon nanotubes dispersed in polyethylenimine as detectors in flow systems, Anal. Chim. Acta 596 (2007) 183–194.
[25] F. Jia, C. Shan, F. Li, L. Niu, Carbon nanotube/gold nanoparticles/polyethylenimine-functionalized ionic liquid thin film composites for glucose, Biosens. Bioelectron. 24 (2008) 945–950.
[26] R. Lopez-Medrano, M.C. Ovejero, J.A. Calera, P. Puente, F. Leal, An immunodominant 90-kilodalton *Aspergillus fumigatus* antigen is the subunit of a catalase, Infect. Immun. 63 (1995) 4774–4780.
[27] Y.C. Tsai, J.M. Chen, S.C. Li, F. Marken, Electroanalytical thin film electrodes based on a Nafion™—multi-walled carbon nanotube composite, Electrochem. Commun. 6 (2004) 917–922.
[28] M.M. Bradford, A rapid and sensitive method for the quantification of microgram quantities of protein utilizing the principle of protein dye binding, Anal. Biochem. 72 (1976) 248–254.
[29] F. Lisdat, D. Schafer, The use of electrochemical impedance spectroscopy for biosensing, Anal. Bioanal. Chem. 391 (2008) 1555–1567.
[30] A. Diaz, V.J. Valdes, E. Rudino-Pinera, E. Horjales, W. Hansberg, Structure–function relationships in fungal large-subunit catalases, J. Mol. Bio. 386 (2009) 218–232.
[31] Z. Zhang, S. Chouchane, R.S. Magiliozzo, J.F. Rusling, Direct voltammetry and catalysis with *Mycobacterium tuberculosis* catalaseperoxidase, peroxidases and catalase in lipid films, Anal. Chem. 74 (2002) 163–170.
[32] L. Shen, N. Hu, Heme protein films with polyamidoamine dendrimer: direct electrochemistry and electrocatalysis, Biochim. Biophys. Acta 1608 (2004) 23–33.
[33] H. Lu, Z. Li, N. Hu, Direct voltammetry and electrocatalytic properties of catalase incorporated in polyacrylamide hydrogel films, Biophys. Chem. 104 (2003) 623–632.
[34] H. Huang, N. Hu, Y. Zeng, G. Zhou, Electrochemistry and electrocatalysis with heme proteins in chitosan biopolymer films, Anal. Biochem. 308 (2002) 141–151.
[35] P. Rahimi, H.A. Rafiee-Pour, H. Ghourchian, P. Norouzi, M.R. Ganjali, Ionic liquid/NH_2-MWCNTs as a highly sensitive nano-composite for catalase, Biosens. Bioelectron. 25 (2010) 1301–1306.
[36] A. Salimi, E. Sharifi, A. Noorbakhsh, S. Soltanian, Direct electrochemistry and electrocatalytic activity of catalase immobilized onto electrodeposited nano-scale islands of nickel oxide, Biophys. Chem. 125 (2007) 540–548.
[37] P.A. Prakash, U. Yogeswaran, S.M. Chen, Direct electrochemistry of catalase at multiwalled carbon nanotubes-nafion in presence of needle shaped DDAB for H_2O_2 sensor, Talanta 78 (2009) 1414–1421.
[38] E. Laviron, General expression of the linear potential sweep voltammogram in the case of diffusionless electrochemical systems, J. Electroanal. Chem. 101 (1979) 19–28.
[39] H. Zhou, T.H. Lu, H.X. Shi, Z.H. Dai, X.H. Huang, Direct electrochemistry and electrocatalysis of catalase immobilized on multi-wall carbon nanotubes modified glassy carbon electrode and its application, J. Electroanal. Chem. 612 (2008) 173–178.

[40] B. Zhang, Z. Zhang, B. Wang, J. Yan, J. Li, S.M. Cai, Preparation of gold nano-arraied electrode on silicon substrate and its electrochemical properties: probe into biosensor based on electroluminescence of porous silicon, Acta Chimi. Sin. 59 (2001) 1932–1936.
[41] F.A. Armstrong, H.A. Heering, J. Hirst, Reactions of complex metalloproteins studied by protein-film voltammetry, Chem. Soc. Rev. 26 (1997) 169–179.
[42] A.W. Bott, W.R. Heineman, Chronocoulometry, Curr. Separat. 20 (2004) 121–126.
[43] A. Salimi, A. Noorbakhsh, M. Ghadermarz, Direct electrochemistry and electrocatalytic activity of catalase incorporated onto multiwall carbon nanotubes-modified glassy carbon electrode, Anal. Biochem. 344 (2005) 16–24.
[44] H.J. Jiang, H. Yang, D.L. Akins, Direct electrochemistry and electrocatalysis of catalase immobilized on a SWNT-nanocomposite film, J. Electroanal. Chem. 623 (2008) 181–186.